

# Cluster-Based Normalization Layer for Neural Networks

Bilal FAYE<sup>1</sup>, Hanane AZZAG<sup>2</sup>, Mustapha Lebbah<sup>3</sup>

e-mail: faye@lipn.univ-paris13.fr, azzag@univ-paris13.fr, mustapha.lebbah@uvsq.fr

**Abstract**—Deep learning grapples with challenges in training neural networks, notably internal covariate shift and label shift. Conventional normalization techniques like Batch Normalization (BN) partially mitigate these issues but are hindered by constraints such as dependency on batch size and distribution assumptions. Similarly, mixture normalization (MN) encounters computational barriers in handling diverse Gaussian distributions. This paper introduces Cluster-based Normalization (CB-Norm), presenting two variants: Supervised Cluster-based Normalization (SCB-Norm) and Unsupervised Cluster-based Normalization (UCB-Norm), offering a pioneering single-step normalization strategy. CB-Norm employs a Gaussian mixture model to address gradient stability and learning acceleration challenges. SCB-Norm utilizes predefined data partitioning, termed clusters, for supervised normalization, while UCB-Norm adaptively clusters neuron activations during training, eliminating reliance on predefined partitions. This approach simultaneously tackles clustering and resolution tasks within neural networks, reducing computational complexity compared to existing methods. CB-Norm outperforms traditional techniques like BN and MN, enhancing neural network performance across diverse learning scenarios. Our code implementation is available on our GitHub repository: <https://github.com/b-faye/cluster-based-norm>

## I. INTRODUCTION

Normalization in the context of deep learning is a fundamental data transformation process aimed at conferring specific statistical properties upon the data. Within the domain of data normalization, various techniques are employed, such as centering, scaling, standardizing, decorrelating, and whitening [1]. In deep neural networks (DNNs), input normalization plays a crucial role during training by eliminating the disparities in feature magnitudes. While this normalization process expedites the convergence of neural networks with a single hidden layer [2], its effectiveness in accelerating convergence in networks with multiple hidden layers is not guaranteed. This is attributed to the transformation of data by each layer, leading to activations that may not necessarily retain the same properties as the normalized inputs. From this perspective, the normalization of activations during training emerges as a pivotal strategy to maintain the advantages associated with normalizing inputs. By ensuring that activations maintain a consistent statistical distribution across layers, deep neural networks can benefit from stable and efficient training, ultimately leading to improved model performance.

Batch Normalization (BN), as introduced by Ioffe and Szegedy in their seminal work [3], stands out as the prevailing and widely adopted method for the normalization of activations. BN achieves this by standardizing activations

using batch statistics, which facilitates the utilization of higher learning rates. Nevertheless, BN exhibits limitations tied to batch size dependence and the assumption of uniform data distribution. To mitigate these limitations, specialized variants of BN have been developed (Layer Normalization, Group Normalization, Instance Normalization, etc.) [4]–[23], focusing on addressing issues related to batch size. On a different front, Mixture Normalization (MN) [24] offers an alternative approach, aiming to overcome the constraints imposed by data distribution assumptions. In stark contrast to BN, MN accommodates data samples drawn from diverse distributions. It employs the Expectation-Maximization (EM) algorithm [25] for data clustering based on components, allowing for the normalization of each sample using component-specific statistics. MN’s distinctive approach enhances convergence, particularly in convolutional neural networks, when compared to BN. However, the incorporation of the EM algorithm in mixture models may entail a notable increase in computational time, potentially hampering overall efficiency. This stems from the necessity of estimating parameters across the entire dataset prior to neural network training, ensuring the provision of normalization parameters.

To address this issues, we propose a new normalization method that we named Cluster-based Normalization (CB-Norm). CB-Norm serves as a normalization layer within deep neural network architectures. Building upon the premise that activations mimic a Gaussian mixture model (GMM) [3], CB-Norm assigns parameters to each mixture component as neural network weights. It utilizes these parameters to normalize activations throughout training. These mixture component parameters, serving as weights of the neural network, undergo updates during backpropagation, aligning with the target task and thereby aiding in minimizing the loss. To operationalize this strategy, we suggest two approaches: a supervised version (SCB-Norm) and an unsupervised version (UCB-Norm).

SCB-Norm utilizes pre-defined partitions (clusters) on inputs before neural network training. Each input is assigned to a single cluster, where a cluster represents a grouping of similar data points. These clusters are constructed using domain knowledge. In this setup, each cluster in the input space corresponds to a component in the activation space mixture. As a result, activations from inputs within the same cluster are normalized using the same parameters, specifically the parameters of the component corresponding to the cluster. This method resolves the issue of BN, which estimates parameters from random batches, possibly

including unrelated data.

Unlike SCB-Norm, UCB-Norm doesn't rely on clusters constructed from inputs to build mixture components according to clusters. UCB-Norm only takes the number of mixture components as a hyperparameter, with parameters for each component estimated during neural network training, incorporating input contributions via activations. This approach resolves the use of the costly EM algorithm on the MN with normalization parameters that are no longer constant as in MN, but are updated to better match the changing distribution of activations with network weight updates.

The choice of a Gaussian distribution assumption is justified by its mathematical convenience, flexibility, and ability to approximate diverse data distributions. Additionally, Gaussian distributions align with the Central Limit Theorem and commonly observed data behaviors. GMMs are well-studied, supported by efficient algorithms, and offer simplicity and interpretability.

This study presents four noteworthy contributions:

- **Cluster-Based Normalization (CB-Norm) Advancements:** CB-Norm introduces an approach incrementally learning mixture component parameters during neural network training. Notably, CB-Norm excels in gradient stability, learning acceleration, and adaptability across diverse learning scenarios.
- **Two CB-Norm Applications for Enhanced Normalization:** We present two CB-Norm methods - Supervised Cluster-based Normalization (SCB-Norm), utilizing predefined data partitioning based (clusters), and Unsupervised Cluster-based Normalization (UCB-Norm), which incrementally clusters during training for increased flexibility.
- **Versatile Application in Deep Learning Architectures:** CB-Norm exhibits versatility across various deep neural network architectures, including Transformers and Convolutional Neural Networks. It serves as a layer at different depths, expediting training processes and improving generalization performance consistently.
- **Integration Recommendations for Improved Performance:** We recommend integrating CB-Norm into domains such as domain adaptation and Generative Adversarial Networks (GANs). CB-Norm addresses challenges in domain adaptation effectively, enhancing model performance across diverse data distributions. Additionally, CB-Norm addresses "mode collapse" in GANs and enhances their ability to learn from various modes, as demonstrated by multiple experiments.

## II. RELATED WORK

### A. Batch Normalization

To ensure clear understanding and consistency in our model, and to facilitate comparison with existing work, we adopt the same notations as those used in [24]. In a

convolutional neural network layer, let  $x \in \mathbb{R}^{N \times C \times H \times W}$  represent the neuron's activation, where  $N$ ,  $C$ ,  $H$ , and  $W$  denote batch, channel, height, and width axes. Batch normalization (BN) [3] standardizes  $x$  with  $m$  samples mini-batch  $B = \{x_{1:m} : m \in [1, N] \times [1, H] \times [1, W]\}$ , flattening  $x$  except the channel axis, as follows:

$$\hat{x}_i = \frac{x_i - \mu_B}{\sqrt{\sigma_B^2 + \epsilon}}, \quad (1)$$

where  $\mu_B = \frac{1}{m} \sum_{i=1}^m x_i$  and  $\sigma_B^2 = \frac{1}{m} \sum_{i=1}^m (x_i - \mu_B)^2$  represent the mean and variance, while  $\epsilon > 0$  serves as a small value to mitigate numerical instability. To mitigate the constraints imposed by standardization, BN introduces learnable parameters  $\gamma$  and  $\beta$  to remove the linear regime of nonlinearity in certain activations:

$$\tilde{x}_i = \gamma \hat{x}_i + \beta \quad (2)$$

When the samples in the mini-batch originate from the same distribution, the transformation described in Equation 1 yields a distribution with a mean of zero and a variance of one. This constraint of zero mean and unit variance serves to stabilize the activation distribution, ultimately aiding in the training process.

While BN demonstrates effective performance, it exhibits two notable limitations: its reliance on batch size, leading to suboptimal performance with small batches, and the simplistic assumption that sample within the mini-batch are from the same distribution, a scenario rarely encountered in real-world data. In response to these challenges, several alternative approaches have been introduced.

### B. Extensions of Batch Normalization

Several extensions to batch normalization (BN) have been introduced, including Layer Normalization (LN) [5], Instance Normalization (IN) [7], Group Normalization (GN) [6], and Mixture Normalization (MN) [24]. These variants all employ the common transformation  $x \rightarrow \hat{x}$ , which is applied to the flattened  $x$  along the spatial dimension  $L = H \times W$ , as follows:

$$v_i = x_i - \mathbb{E}_{B_i}(x), \quad \hat{x}_i = \frac{v_i}{\sqrt{\mathbb{E}_{B_i}(v^2) + \epsilon}}, \quad (3)$$

where  $B_i = \{j : j_N \in [1, N], j_C \in [i_C], j_L \in [1, L]\}$ , and  $i = (i_N, i_C, i_L)$  a vector indexing the activations  $x \in \mathbb{R}^{N \times C \times L}$ .

**Layer Normalization (LN):** Alleviates inter-dependency among batch-normalized activations by computing mean and variance using input from individual layer neurons. LN proves beneficial for recurrent networks but can encounter difficulties with convolutional layers due to spatial variations in visual data. It can be formulated as Equation 3 when  $B_i = \{j : j_N \in [i_N], j_C \in [1, C], j_L \in [1, L]\}$ .

**Instance Normalization:** A normalization approach that normalizes each sample individually, primarily aimed at eliminating style information, particularly

in images. IN enhances the performance of specific deep neural networks (DNNs) by computing mean values and standard deviations in the spatial domain. It finds extensive use in applications such as image style transfer [26] [27]. It can be formulated as Equation 3 when  $B_i = \{j : j_N \in [i_N], j_C \in [i_C], j_L \in [1, L]\}$ .

**Group Normalization (GN):** A normalization method that partitions neurons into groups and autonomously standardizes layer inputs for each sample within these groups. GN performs exceptionally well in visual tasks characterized by small batch sizes, such as object detection and segmentation. GN partitions the channels into several groups ( $G$ ), calculating statistics along the  $L$  axis, but restricting this computation to subgroups of the channels. When  $G = C$ , GN is equivalent to IN, and it is identical to LN when  $G = 1$ .

**Mixture Normalization (MN):** In the realm of deep neural networks (DNNs), the distribution of activations inherently encompasses multiple modes of variation due to the presence of non-linearities. The batch normalization (BN) [3] assumption that a Gaussian distribution suffices to model the generative process of mini-batch samples becomes less applicable. In response, Mixture Normalization (MN) [24] approaches BN from the perspective of Fisher kernels, originating from generative probability models. Instead of computing mean and standard deviation across entire instances within a mini-batch, MN employs a Gaussian Mixture Model (GMM) to assign each instance in the mini-batch to a component and subsequently normalizes with regard to multiple means and standard deviations associated with different modes of variation in the underlying data distribution.

MN normalizes each sample within the mini-batch by utilizing the mean and standard deviation corresponding to the mixture component to which the sample is assigned. The probability density function  $p_\theta$  that characterizes the data can be represented as a parameterized Gaussian Mixture Model (GMM). Let  $x \in \mathbb{R}^D$ , and  $\theta = \{\lambda_k, \mu_k, \Sigma_k : k = 1, \dots, K\}$ ,

$$p(x) = \sum_{k=1}^K \lambda_k p(x|k), \text{ s.t. } \forall_k : \lambda_k \geq 0, \sum_{k=1}^K \lambda_k = 1, \quad (4)$$

where

$$p(x|k) = \frac{1}{(2\pi)^{D/2} |\Sigma_k|^{1/2}} \exp\left(-\frac{(x - \mu_k)^T \Sigma_k^{-1} (x - \mu_k)}{2}\right), \quad (5)$$

is the  $k^{th}$  Gaussian in the mixture model  $p(x)$ ,  $\mu_k$  the mean vector and  $\Sigma_k$  is the covariance matrix.

The probability that  $x$  has been generated by the  $k^{th}$  Gaussian component in the mixture model can be defined as:

$$\tau_k(x) = p(k|x) = \frac{\lambda_k p(x|k)}{\sum_{j=1}^K \lambda_j p(x|j)}, \quad (6)$$

Based on these assumptions and the general transform in Equation (3), the Mixture Normalizing Transform for a given

$x_i$  is defined as

$$\hat{x}_i = \sum_{k=1}^K \frac{\tau_k(x_i)}{\sqrt{\lambda_k}} \hat{x}_i^k, \quad (7)$$

given

$$v_i^k = x_i - \mathbb{E}_{B_i}[\hat{\tau}_k(x).x], \quad \hat{x}_i^k = \frac{v_i^k}{\sqrt{\mathbb{E}_{B_i}[\hat{\tau}_k(x).(v^k)^2] + \epsilon}}, \quad (8)$$

where

$$\hat{\tau}_k(x_i) = \frac{\tau_k(x_i)}{\sum_{j \in B_i} \tau_k(x_j)}, \quad (9)$$

is the normalized contribution of  $x_i$  with respect to the mini-batch  $B_i = \{j : j_N \in [i_N], j_C \in [i_C], j_L \in [1, L]\}$  in the estimation of the statistical measures of the  $k^{th}$  Gaussian component.

With this approach, Mixture Normalization can be implemented in two stages:

- Estimation of the mixture model's parameters  $\theta = \{\lambda_k, \mu_k, \Sigma_k : k = 1, \dots, K\}$  using the Expectation-Maximization (EM) algorithm [25].
- Normalization of each sample based on the estimated parameters (see Equation (8)) and aggregation using posterior probabilities (see Equation (7)).

In the context of convolutional neural networks, this method enables Mixture Normalization to outperform batch normalization in terms of convergence and accuracy in supervised learning tasks.

### III. PROPOSED METHOD: CLUSTER-BASED NORMALIZATION

To address the issues related to the naive assumption of batch normalization, which assumes that data within mini-batch are from the same distribution, and to overcome the computational cost of mixture normalization due to the use of the EM algorithm to find the parameters of each component of the Gaussian mixture, our method, Cluster-based Normalization (CB-Norm), operates in three steps:

- As outlined in [3], CB-Norm operates under the assumption that activations can be represented by a Gaussian mixture model. During neural network training, CB-Norm calculates the parameters of each Gaussian component.
- During neural network training, activations are normalized using estimated Gaussian component parameters in two distinct ways: supervised (SCB-Norm) and unsupervised (UCB-Norm). This approach effectively resolves the distribution hypothesis of batch normalization.
- The parameters of Gaussian components serve as weights in the neural network, thus aiding in minimizing the loss function and are updated during the backpropagation process. This method eliminates the necessity of the EM algorithm in mixture normalization by employing an end-to-end approach to learn the

parameters of mixture components and simultaneously train the neural network.

### A. Supervised Cluster-based Normalization (SCB-Norm)

In SCB-Norm, the composition of mixture components is guided by prior knowledge, termed "clusters", which represent groups of input data sharing similar traits. The formation of clusters relies on domain-specific knowledge of the dataset. For instance, in domain adaptation, the source and target domains can be treated as separate clusters. Each cluster, denoted by  $z \in \{1, \dots, Z\}$ , corresponds to a mixture component, represented by  $k \in \{1, \dots, K\}$ , within the activation space. Here,  $Z$  and  $K$  respectively represent the number of clusters and the number of mixture components, with  $Z$  being equal to  $K$ . Activations from data inputs within the same cluster are normalized using the same parameters, which are the parameters of the corresponding mixture component. For a specific input indexed by  $i$ , it is denoted as  $(x_i, z_i)$ , where  $x_i$  represents the data and  $z_i \in \{1, \dots, Z\}$  is the cluster identifier indicating the cluster to which the input belongs.

To reduce the number of parameters that need to be learned, we operate under the assumption that clusters have equal probabilities, hence the mixture coefficients are constant for all  $k \in \{1, \dots, K\}$ . Consequently, we only need to learn the parameters  $\{\mu_k, \sigma_k^2\}_{k=1}^K$ .

Let  $x$  represent an activation tensor in  $\mathbb{R}^{N \times C \times H \times W}$ . Define  $B_i = \{j : j_N \in [i_N], j_C \in [i_C], j_L \in [1, L]\}$ , encompassing all activations in  $x$  on the channel  $i$ , where  $x$  is flattened along the  $L = H \times W$  axis. In SCB-Norm, each  $x_i$  within  $B_i$  is normalized using a function  $f$  as follows:

$$f_{\theta_{k_i}}(x_i) : \hat{x}_i \leftarrow \frac{x_i - \mu_{k_i}}{\sqrt{\sigma_{k_i}^2 + \epsilon}}, \quad (10)$$

where  $\theta_{k_i} = \{\mu_{k_i}, \sigma_{k_i}^2\}$  represents the parameters of the mixture component  $k$  to which  $x_i$  belongs. This component corresponds to a cluster  $z$  in the input space, where the transformation of input data to the latent space results in the activation  $x_i$ .

During neural network training, activations are normalized using Equation 10. The parameters of the mixture components, serving as weights in the neural network, are iteratively updated based on the overall loss of the neural network. This update process aims to minimize the loss, consequently improving the performance of the neural network, as depicted in Algorithm 1. It is essential to calculate gradients concerning the parameters of the SCB-Norm transformation. When considering  $\ell$ , the total loss of the neural network, this gradient computation requires the application of the chain rule, as shown in the upcoming expression (before any simplifications):

$$\begin{cases} \frac{\partial \ell}{\partial \mu_{k_i}} = -\frac{\partial \ell}{\partial \hat{x}_i} \cdot (\sigma_{k_i}^2 + \epsilon)^{-1/2} \\ \frac{\partial \ell}{\partial \sigma_{k_i}^2} = \frac{\partial \ell}{\partial \hat{x}_i} \cdot \frac{\mu_{k_i} + x_i}{2(\sigma_{k_i}^2 + \epsilon)^{3/2}} \end{cases} \quad (11)$$

---

### Algorithm 1: Training an Supervised Cluster-based Network

---

**Input :** Deep neural network  $Net$  with trainable parameters  $\Theta$ ; subset of activations and its clusters  $\{x_i, k_i\}_{i=1}^m$ , with  $k_i \in \{1, \dots, K\}$ , where  $K$  is the number of mixture components

**Output:** Supervised Cluster-based Normalized deep neural network for inference,  $Net_{SCB-Norm}^{inf}$

- 1  $Net_{SCB-Norm}^{tr} = Net$  // Training SCB-Norm deep neural network
- 2 **for**  $i \leftarrow 1$  to  $m$  **do**
  - Add transformation  $\hat{x}_i = f_{\theta_{k_i}}(x_i)$  to  $Net_{SCB-Norm}^{tr}$  (Equation 10)
  - Modify each layer in  $Net_{SCB-Norm}^{tr}$  with input  $x_i$  to take  $\hat{x}_i$  instead
- 3 **end**
- 4 Train  $Net_{SCB-Norm}^{tr}$  to optimize the parameters:  $\Theta = \Theta \cup \{\mu_k, \sigma_k\}_{k=1}^K$
- 5  $Net_{SCB-Norm}^{inf} = Net_{SCB-Norm}^{tr}$  // Inference SCB-Norm network with frozen parameters
- 6 **for**  $i \leftarrow 1$  to  $m$  **do**
  - 7 **if**  $k_i$  is known **then**
    - normalize  $x_i$  using Equation 10
  - 8 **end**
  - 9 **else**
    - normalize  $x_i$  using Equation 12
  - 10 **end**
- 11 **end**

---

SCB-Norm functions as a differentiable operation within deep neural networks, facilitating the normalization of activations. This adaptability ensures that neural network representations evolve continuously to suit the target task, thereby improving overall performance. By mitigating variations in activation distributions, the normalization process enables the model to emphasize relevant patterns and features more effectively.

During inference, there are two scenarios for applying SCB-Norm. If the cluster  $z$  of a given input data is known, the resulting activations are normalized using the corresponding mixture component parameters  $k$ , applying Equation 10. However, if the cluster of the input data is unknown, normalization is conducted across all mixture components by adapting Equation 7 as follows:

$$\hat{x}_i = \sqrt{K} \sum_{k=1}^K \tau_k(x_i) \hat{x}_i^k, \quad (12)$$

with

$$\tau_k(x_i) = p(k|x_i) = \frac{p(x_i|k)}{K \sum_{j=1}^K p(x_i|j)}, \quad \hat{x}_i^k = \frac{x_i - \mu_k}{\sigma_k}, \quad (13)$$



assuming that the prior probabilities ( $\lambda_k = \frac{1}{K}, k = 1, \dots, K$ ) are constant.

### B. Unsupervised Cluster-based Normalization (UCB-Norm)

In UCB-Norm, we take a different approach by not relying on prior knowledge (clusters). Instead, the neural network autonomously discovers a latent space over activations that adheres to a GMM. UCB-Norm incrementally clusters neuron activations during training without predefined partitions. This allows the model to adapt to task-specific challenges without relying on prior cluster information. The absence of predefined partitions provides UCB-Norm with increased flexibility, as it allows the neural network to explore and adapt to patterns in the data on its own.

Since the specific mixture component to which a given activation belongs is unknown, UCB-Norm employs Equation 7, which normalizes across all components. Unlike MN, the parameters of these components are learned as

neural network weights during backpropagation, eliminating the need for computationally expensive algorithms like EM. The number of mixture components, denoted as  $K$ , acts as a hyperparameter.

During training, the update of mixture component parameters involves two approaches (see Algorithm 2): one aligns updates with the target task, enhancing specialization and optimization for improved task-specific learning and generalization. The second approach estimates parameters using moving averages within each batch, offering stability, robustness, and regularization. This dual strategy combines task-aligned updates and moving averages for effective and versatile training.

In the context of UCB-Norm, computing gradients with respect to the transformation parameters is crucial for optimizing the neural network. This involves applying the chain rule to the total loss  $\ell$ , as demonstrated in the forthcoming expression (prior to any simplifications):

$$\begin{aligned}
\frac{\partial \ell}{\partial \lambda_k} &= \frac{\partial \ell}{\partial \hat{x}_i} \sum_{k=1}^K \frac{\partial \ell}{\partial \lambda_k} \left( \frac{\tau_k(x_i)}{\sqrt{\lambda_k}} \hat{x}_i^k \right) \\
&= \frac{\partial \ell}{\partial \hat{x}_i} \sum_{k=1}^K \frac{\partial \ell}{\partial \lambda_k} \left( \frac{\tau_k(x_i)}{\sqrt{\lambda_k}} \right) \hat{x}_i^k + \frac{\tau_k(x_i)}{\sqrt{\lambda_k}} \frac{\partial \ell}{\partial \lambda_k} \left( \frac{v_i^k}{\sqrt{\mathbb{E}_{B_i}[\hat{\tau}_k(x)(v^k)^2] + \epsilon}} \right) \\
\frac{\partial \ell}{\partial \mu_k} &= \frac{\partial \ell}{\partial \hat{x}_i} \sum_{k=1}^K \frac{\partial \ell}{\partial \mu_k} \left( \frac{\tau_k(x_i)}{\sqrt{\lambda_k}} \hat{x}_i^k \right) \\
&= \frac{\partial \ell}{\partial \hat{x}_i} \sum_{k=1}^K \frac{1}{\sqrt{\lambda_k}} \frac{\partial \ell}{\partial \mu_k} (\tau_k(x_i)) \hat{x}_i^k + \frac{\tau_k(x_i)}{\sqrt{\lambda_k}} \frac{\partial \ell}{\partial \mu_k} \left( \frac{v_i^k}{\sqrt{\mathbb{E}_{B_i}[\hat{\tau}_k(x)(v^k)^2] + \epsilon}} \right) \\
\frac{\partial \ell}{\partial \sigma_k^2} &= \frac{\partial \ell}{\partial \hat{x}_i} \sum_{k=1}^K \frac{\partial \ell}{\partial \sigma_k^2} \left( \frac{\tau_k(x_i)}{\sqrt{\lambda_k}} \hat{x}_i^k \right) \\
&= \frac{\partial \ell}{\partial \hat{x}_i} \sum_{k=1}^K \frac{1}{\sqrt{\lambda_k}} \frac{\partial \ell}{\partial \sigma_k^2} (\tau_k(x_i)) \hat{x}_i^k + \frac{\tau_k(x_i)}{\sqrt{\lambda_k}} \frac{\partial \ell}{\partial \sigma_k^2} \left( \frac{v_i^k}{\sqrt{\mathbb{E}_{B_i}[\hat{\tau}_k(x)(v^k)^2] + \epsilon}} \right)
\end{aligned} \tag{14}$$

During inference, when the model has converged, the parameters of the mixture components are utilized for normalization:

$$\hat{x}_i \leftarrow \sum_{k=1}^K \frac{\tau_k(x_i)}{\sqrt{\lambda_k}} \left( \frac{x_i - \mu_k}{\sigma_k} \right) \tag{15}$$

This approach significantly reduces complexity compared to MN, which involves processing  $T$  mini-batches, applying EM, and storing the estimated parameters for inference.

### C. Analyzing Computational Complexity In Detail

The computational overhead of cluster-based normalization, when compared to batch normalization and mixture normalization, stems from the task of estimating mixture components parameters. Let  $B$  denote a batch of activations located in  $\mathbb{R}^d$ , where  $d$  signifies the dimensionality of activations.

Batch normalization computes the mean ( $\mu_B$ ) and standard deviation ( $\sigma_B$ ) by considering the entire set of activations within the batch  $B$ . In terms of complexity, this involves calculating the mean ( $\mu$ ) and standard deviation ( $\sigma$ ) for each dimension of the batch (see Equation 1), resulting in a computational complexity of  $\mathcal{O}(d)$ . Additionally, this method requires learning two parameters,  $\gamma$  and  $\beta$ , for each dimension of the batch, contributing to a parameter learning complexity of  $\mathcal{O}(d)$ . Therefore, the overall complexity, considering both computational and parameter aspects, is  $\mathcal{O}(d)$  for the entire batch  $B$ .

The computational challenge associated with mixture normalization arises from the intricate process of accurately estimating the parameters of the GMM. This process involves a two-stage approach, where a seeding procedure is first employed to initialize the centers of the mixture components. Subsequently, the Expectation-Maximization (EM) algorithm is iteratively applied to estimate the

---

**Algorithm 2:** Training an Unsupervised Cluster-based Normalization Network
 

---

**Input :** Deep neural network  $Net$  with trainable parameters  $\Theta$ ; subset of activations  $\{x_i\}_{i=1}^m$ ; number of clusters  $K$ ; momentum  $m$ ;  $update \in \{weight, moving\ average\}$

**Output:** Unsupervised Cluster-based Normalized deep neural network for inference,  $Net_{UCB-Norm}^{inf}$

- 1  $Net_{UCB-Norm}^{tr} = Net$  // Training UCB-Norm deep neural network
- 2 Initialize the parameters for each cluster as follows:  $(\lambda_k, \mu_k, \sigma_k^2)$  for  $k \in \{1, \dots, K\}$ , subject to the conditions that  $\sum_{k=1}^K \lambda_k = 1$  and  $\sigma_k^2 > 0$  for all  $k \in \{1, \dots, K\}$ .
- 3 **for**  $i \leftarrow 1$  **to**  $m$  **do**
  - Add transformation  $\hat{x}_i$  using Equation 7
  - Modify each layer in  $Net_{UCB-Norm}^{tr}$  with input  $x_i$  take  $\hat{x}_i$  instead
- 4 **end**
- 5 **if**  $update = weight$  **then**
  - 6 // Update parameters as weights of the neural network
  - 7 Train  $Net_{UCB-Norm}^{tr}$  to optimize the parameters:  $\Theta = \Theta \cup \{\lambda_k, \mu_k, \sigma_k\}_{k=1}^K$
- 8 **end**
- 9 **if**  $update = moving\ average$  **then**
  - 10 // Update parameters using moving average according the batch
  - 11 **for**  $r \leftarrow 1$  **to**  $K$  **do**
    - 12  $\lambda_k \leftarrow m \times \lambda_k + (1 - m) \times mean(\tau_k)$
    - 13  $\mu_k \leftarrow m \times \mu_k + (1 - m) \times mean(\hat{x}^k)$
    - 14  $\sigma_k^2 \leftarrow m \times \sigma_k^2 + (1 - m) \times variance(\hat{x}^k)$
  - 15 **end**
- 16 **end**
- 17  $Net_{UCB-Norm}^{inf} = Net_{UCB-Norm}^{tr}$  // Inference UCB-Norm network with frozen parameters
- 18 **for**  $i \leftarrow 1$  **to**  $m$  **do**
  - Add transformation  $\hat{x}_i$  using Equation 15
  - Modify each layer in  $Net_{UCB-Norm}^{inf}$  with input  $x_i$  take  $\hat{x}_i$  instead
- 19 **end**

---

parameters of the mixture model. In mixture normalization, K-means++ [28] is specifically chosen as the seeding procedure due to its applicability without assuming any characteristics about the underlying data. The complexity of the K-means++ algorithm for a given batch  $B$  of samples with dimension  $d$  is  $\mathcal{O}(d \cdot K \cdot \log(k))$ , where  $K$  is the number of mixture component centers. For the EM algorithm, the complexity of each iteration is  $\mathcal{O}(d \cdot n \cdot K)$ , where  $n$  is the number of samples in  $B$ . The EM algorithm typically converges in a small number of iterations, often less than 10 or 20. Consequently, the overall complexity of running K-means++ followed by the EM algorithm on a batch of samples  $B$  is primarily determined by the

initialization step, resulting in  $\mathcal{O}(d \cdot K \cdot \log(K))$ , with an additional contribution from the EM iterations. The total number of iterations for the EM algorithm depends on the convergence criteria and the specific characteristics of the data. In practice, the overall complexity is often dominated by the initialization step for K-means++.

For our cluster-based normalization approach, we will detail the complexity for the supervised version (SCB-Norm) and the unsupervised version (UCB-Norm). Consider the batch  $B$ , with dimension  $d$ . Assuming that the defined number of prior knowledge (clusters) is  $Z = K$ , the complexity of SCB-Norm is correlated with  $K$ . Specifically, for each mixture component  $k$ , two learnable parameters of dimension  $d$  are associated with it ( $\mu_k$  and  $\sigma_k^2$ ). Therefore, the total number of parameters to be learned for all mixture components is  $2 \times K \times d$ , resulting in a complexity of  $\mathcal{O}(K \cdot d)$  for SCB-Norm. The unsupervised version, UCB-Norm, estimates three learnable parameters for each mixture component  $K$ :  $\lambda_k$  of dimension 1, and  $\mu_k$  and  $\sigma_k$  of dimension  $d$ . This results in a total of  $2 \times K \times d + K$  parameters to be learned, with a complexity of  $\mathcal{O}(K \cdot d)$ . Unlike mixture normalization, both the supervised and unsupervised versions of cluster-based normalization are performed in a one-stage process, and the complexity is solely associated with the parameter estimation during the backpropagation process. A detailed comparison is presented in Table I.

#### IV. EXPERIMENTS

In the upcoming experiments, we plan to evaluate how well the Cluster-based Normalization (CB-Norm) performs and to conduct a comparison with Batch Normalization (BN) and Mixture Normalization (MN).

We suggest applying both implementations of CB-Norm: Supervised version (SCB-Norm) and Unsupervised version (UCB-Norm)—to tasks involving classification (Section IV-B, IV-C and IV-F), domain adaptation (Section IV-E), and generative neural networks (Section IV-D).

In addition to SCB-Norm, we will incorporate a variant known as SCB-Norm-base. In SCB-Norm-base, two separate neural layers estimate the  $K$  mixture components parameters  $\theta = \{\mu_k, \sigma_k\}_{k=1}^K$ . For a given activation  $x_i$  in the SCB-Norm-base layer, the component identifier  $k_i$  of  $x_i$  is initially encoded using one-hot encoding and serves as input for both layers. The first layer outputs  $\mu_{k_i}$ , while the second provides  $\sigma_{k_i}^2$ , which are then used to normalize  $x_i$ .

Detailed descriptions of the methods under consideration are provided in Table II.

##### A. Datasets

The experiments in this study make use of several benchmark datasets that are widely recognized within the classification community:

- **CIFAR-10:** A dataset with 50,000 training images and 10,000 test images, each of size  $32 \times 32$  pixels, distributed across 10 classes [29].

| Normalization Method                                | Computational Complexity         | Parameter Complexity     |
|---|----------------------------------|--------------------------|
| Batch Normalization (BN)                            | $\mathcal{O}(d)$                 | $\mathcal{O}(d)$         |
| Mixture Normalization (MN)                          | $\mathcal{O}(d \cdot n \cdot K)$ | $\mathcal{O}(d)$         |
| Supervised Cluster-based Normalization (SCB-Norm)   | 0                                | $\mathcal{O}(K \cdot d)$ |
| Unsupervised Cluster-based Normalization (UCB-Norm) | 0                                | $\mathcal{O}(K \cdot d)$ |

**TABLE I:** Complexities in Estimating Parameters for Normalization Methods. Computational Complexity corresponds to the time required for parameter estimation, while Parameter Complexity corresponds to the number of parameters to be estimated. Here,  $d$  represents the dimension of the data,  $K$  denotes the number of mixture component centers, and  $n$  the number of samples.

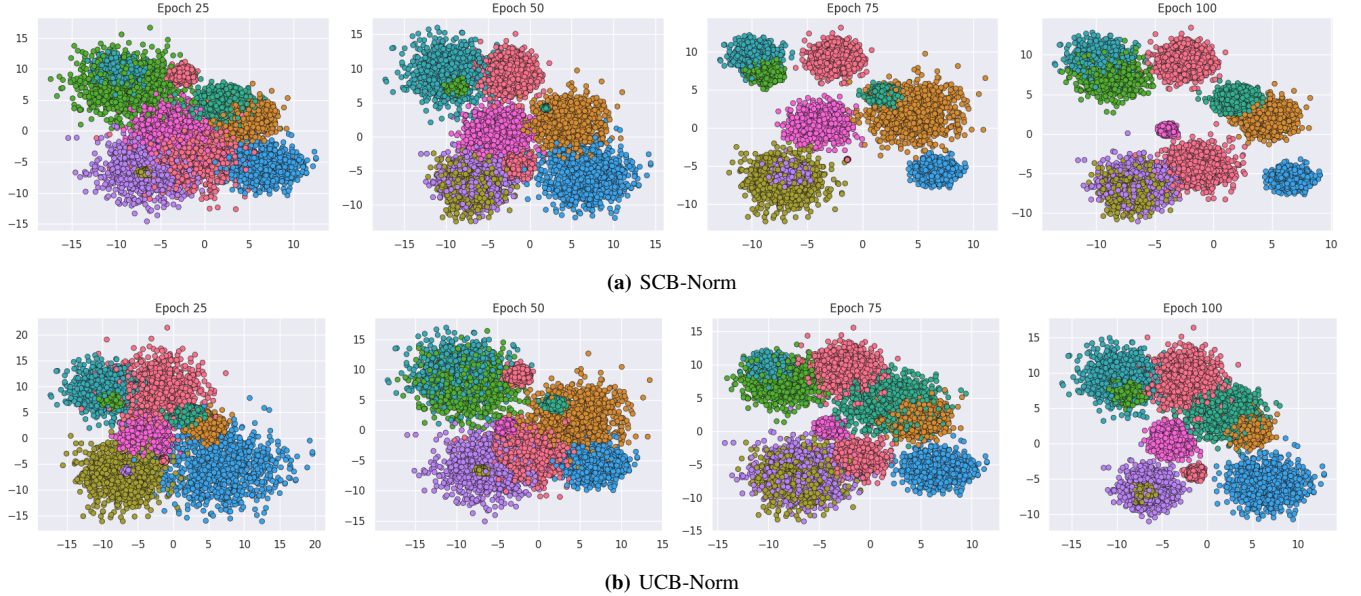


**Fig. 1:** Visualization of Clustering Patterns in Activations: The t-SNE visualization of activations from models trained on CIFAR-10 with SCB-Norm and UCB-Norm normalization layers. The figure illustrates the formation of distinct mixture components aligning with predicted target classes, showcasing improved clustering patterns over the course of training.

| Normalization Layer | Description  |
|---------------------|--|
| BN                  | Layer with batch normalizing transform (ref. Section II-A)   |
| MN                  | Layer with mixture normalizing transform (ref. Section II-B)   |
| SCB-Norm            | Layer with supervised cluster-based normalization transform (ref. Algorithm 1)   |
| SCB-Norm-base       | A softened version of SCB-Norm involves employing two distinct layers to independently learn $\mu$ and $\sigma$ for all mixture components. The cluster identifier one-hot encoding $onehot(k)$ serves as input for both layers. |
| UCB-Norm            | Layer with unsupervised cluster-based normalization (ref. Algorithm 2)   |

**TABLE II:** Normalization method used in the experiments

- **CIFAR-100:** Derived from the Tiny Images dataset, it consists of 50,000 training images and 10,000 test images of size  $32 \times 32$ , divided into 100 classes grouped into 20 superclasses [30].
- **Tiny ImageNet:** A dataset that is a reduced version of the ImageNet dataset, containing 200 classes with 500 training images and 50 test images per class [31].
- **MNIST digits:** Contains 70,000 grayscale images of size  $28 \times 28$  representing the 10 digits, with around 6,000 training images and 1,000 testing images per class [32].

- **SVHN:** A challenging dataset with over 600,000 digit images, focusing on recognizing digits and numbers in natural scene images [33].

| Dataset                    | Task  |
|----------------------------|---|
| CIFAR-10 and Tiny ImageNet | This datasets are used for training a shallow convolutional neural network (ref. Section IV-B).   |
| CIFAR-100                  | Three experiments (ref. Sections IV-B, IV-C, and IV-D) involve the use of this dataset. These experiments encompass the training of shallow and deep convolutional neural networks, as well as the training of a generative neural network. |
| MNIST digits and SVHN      | This datasets are used to train the AdaMatch [34] model in unsupervised domain adaptation (ref. Section IV-E).  |

**TABLE III:** Summary of datasets and associated training experiments

Table III provides a visual representation of the mapping between each dataset and the specific experiments in which it is utilized.

### B. A Comparative Study: Cluster-based Normalization vs. Batch Normalization and Mixture Normalization Using Shallow Convolutional Neural Network

In this study, we employ a shallow convolutional neural network (Shallow CNN) structure outlined in Table IV. Five models are constructed based on the Shallow CNN (see

| layer  | type         | size                      | kernel       | (stride, pad) |
|--------|--------------|---------------------------|--------------|---------------|
| input  | input        | $3 \times 32 \times 32$   | -            | -             |
| conv1  | conv+bn+relu | $64 \times 32 \times 32$  | $5 \times 5$ | (1, 2)        |
| pool1  | max pool     | $64 \times 16 \times 16$  | $3 \times 3$ | (2, 0)        |
| conv2  | conv+bn+relu | $128 \times 16 \times 16$ | $5 \times 5$ | (1, 2)        |
| pool2  | max pool     | $128 \times 8 \times 8$   | $3 \times 3$ | (2, 0)        |
| conv3  | conv+bn+relu | $128 \times 8 \times 8$   | $5 \times 5$ | (1, 2)        |
| pool3  | max pool     | $128 \times 4 \times 4$   | $3 \times 3$ | (2, 0)        |
| conv4  | conv+bn+relu | $256 \times 4 \times 4$   | $3 \times 3$ | (1, 1)        |
| pool4  | avg pool     | $256 \times 1 \times 1$   | $4 \times 4$ | (1, 0)        |
| linear | linear       | 10, 100 or 200            | -            | -             |

**TABLE IV:** Shallow CNN Architecture as Described in the Mixture Normalization (MN) Paper: A Comparison of MN and BN under Small and Large Learning Rate Regimes.

Table IV). The first model, denoted as BN, aligns with the foundational architecture of the Shallow CNN, incorporating only Batch Normalization layers for normalization. The remaining four models—MN, SCB-Norm, SCB-Norm-base, and UCB-Norm—are obtained by substituting the third Batch Normalization layer in the Shallow CNN with the respective layers of MN, SCB-Norm, SCB-Norm-base, and UCB-Norm (see Table II). As per the findings in [24], we conduct experiments employing two distinct learning rates, where one is five times larger than the other.

The mini-batch size is fixed at 256, and all models undergo training for 100 epochs using the AdamW optimizer [35,36] with a weight decay of  $1e - 4$ . In the training phase on CIFAR-10, CIFAR-100, and Tiny ImageNet datasets, we utilize the MN method, which entails estimating a Gaussian mixture model through Maximum Likelihood Estimation (MLE). For comparative analysis, the three mixture components identified by the Expectation-Maximization (EM) algorithm on MN serve as separate clusters (prior knowledge) ( $Z = K = 3$ ) for SCB-Norm and SCB-Norm-base. In UCB-Norm, we define the number of mixture components for estimating as  $K = 3$ . Our main goal is not to attain state-of-the-art results, which typically demand computationally expensive architectures and meticulous parameter tuning. Rather, our focus is on illustrating that the replacement or integration of our cluster-based normalization technique (SCB-Norm and UCB-Norm) can enhance the convergence rate, resulting in improved test accuracy. This underscores the substantial impact of our approach in enhancing model performance.

In Figure 2, we illustrate the activation distribution for models employing CB-Norm (SCB-Norm, UCB-Norm) and those without CB-Norm (BN, MN). Models using CB-Norm exhibit a closer resemblance to the normal distribution and display probability densities with reduced skewness. Clearly, CB-Norm provides a more accurate approximation of  $p(x)$ , as shown by the solid green curve, exhibiting a closer alignment with the underlying distribution compared to models without CB-Norm. Figure 5 highlights the swifter convergence of SCB-Norm, its compact variant SCB-Norm-base, and UCB-Norm in comparison to BN and MN. This accelerated convergence translates into enhanced performance on the validation dataset, with an

average accuracy improvement of **2%** on CIFAR-10, **3%** on CIFAR-100, and **4%** on Tiny ImageNet, as detailed in Table V. This positive trend holds consistent across varying class numbers (10, 100, 200), even with an augmented learning rate from 0.001 to 0.005. The widening gap in convergence with the elevated learning rate underscores the effectiveness of our normalization technique in adeptly harnessing higher learning rates during training.

During the training of the Shallow CNN on the CIFAR-10 dataset, we consistently captured snapshots at 25-epoch intervals, integrating both SCB-Norm and UCB-Norm techniques. Following this, the trained models were employed on a randomly chosen CIFAR-10 batch, and the resulting activations underwent t-SNE visualization. The visual representations revealed the formation of clusters closely resembling the target classes predicted by the individual models. Notably, as training progressed, a noticeable refinement in these clusters was observed, contributing to a comprehensive improvement in performance, as depicted in Figure 1.

To substantiate the hypothesis that CB-Norm can significantly contribute to accelerating the convergence of a neural network training, we will employ a Deep Convolutional Neural Network in the following experiment using the CIFAR-100 dataset.

### C. A Comparative Study: Cluster-based Normalization vs. Batch Normalization and Mixture Normalization Using Deep Convolutional Neural Network

We have demonstrated that the incorporation of cluster-based normalization techniques (SCB-Norm, SCB-Norm-base, and UCB-Norm) results in enhanced convergence speed and improved performance in models where batch normalization serves as the baseline layer normalization. It’s worth noting that our experiments were conducted on a relatively shallow architecture comprising only four convolutional layers. This raises a valid question about whether this observed behavior persists in more extensive and contemporary architectures. To investigate this, we select DenseNet [37] as our preferred architecture. We leverage two foundational architectures featuring 40 and 100 layers, aligning with the structure outlined in the mixture normalization paper. These architectures encompass three dense blocks and two transition layers, maintaining a consistent growth rate of 12. DenseNet is characterized by its dense connectivity pattern, where each layer receives direct input from all preceding layers within a dense block. This unique structure promotes feature reuse and enhances model expressiveness. All models undergo 200 epochs of training on the CIFAR-100 dataset, with a batch size of 64 and utilizing Nesterov’s accelerated gradient [38]. The learning rate initiates at 0.1 and is reduced by a factor of 10 at 50% and 75% of the total training epochs. Additionally, weight decay and momentum values are set to  $10^{-4}$  and 0.9, respectively. To compare



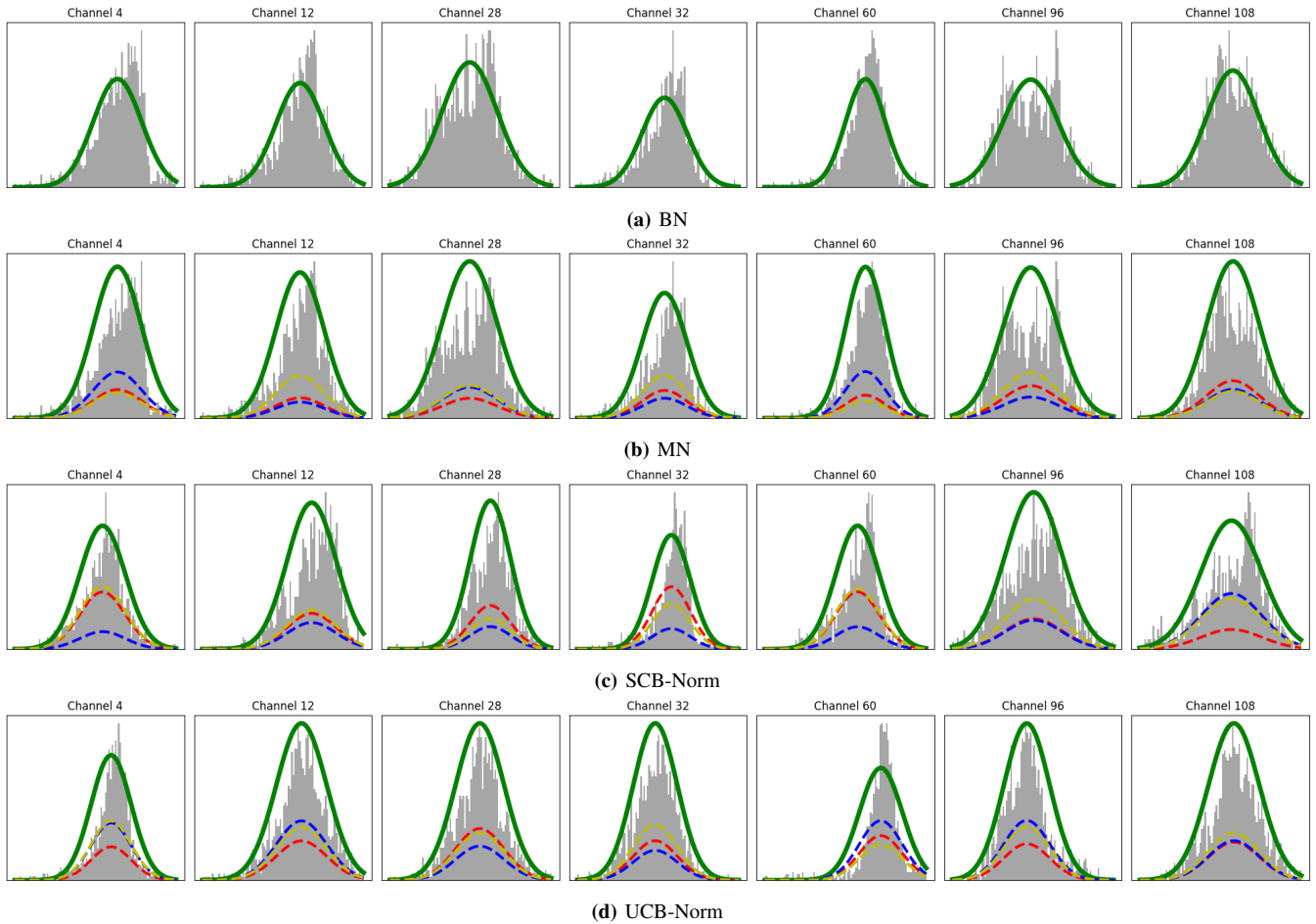


**Fig. 2:** Using a randomly selected mini-batch on CIFAR-100, we depict the distribution of activations related to a subset of 128 channels within the "conv2" layer of the Shallow CNN architecture (specified in Table IV). The solid green curve represents the probability density function, while dashed curves depict distinct mixture components, each distinguished by various colors.

the three normalization methods (batch normalization, mixture normalization, and cluster-based normalization), we create five models for each variant (DenseNet-40 and DenseNet-100). The initial model reflects the foundational structure of DenseNet, featuring Batch Normalization layers exclusively for normalization. The second model mirrors the fundamental DenseNet architecture but introduces the MN layer as the initial layer. Models three through five correspondingly involve integrating SCB-Norm-base, SCB-Norm, and UCB-Norm layers as the initial layer in the base DenseNet model. Placing these normalization layers as the initial layer facilitates the direct infusion of cluster information for adaptive normalization directly into the image. In the case of constructing components with MN, we set  $K = 5$ . Additionally, components derived from the EM algorithm are regarded as prior clusters ( $Z = K = 5$ ) for SCB-Norm-base and SCB-Norm. For the unsupervised version of CB-Norm, we also adopt  $K = 5$  for the number of mixture components.

Throughout the CIFAR-100 training regimen, we systematically recorded snapshots at intervals of 25 epochs, incorporating the SCB-Norm and UCB-Norm techniques.

Subsequently, the trained models were applied to a randomly selected CIFAR-100 batch, and the resulting activations underwent t-SNE visualization. The visual representations exposed the emergence of clusters closely mirroring the target classes predicted by the respective models. Notably, a discernible refinement in these clusters was observed with progressive training, contributing to a comprehensive performance enhancement, as illustrated in Figure 9.

Figure 8 vividly demonstrates that the integration of CB-Norm (SCB-Norm-base, SCB-Norm, and SCB-Norm) goes beyond simply expediting optimization during training—it consistently yields superior generalization across different architectural configurations. This advantage becomes particularly pronounced in the more intricate setting of the DenseNet architecture. Utilizing DenseNet with 40 layers (DenseNet-40) on CIFAR-100, the test error for the Batch Normalization (BN) and Mixture Normalization (MN) variants stands at **0.38** and **0.37**, respectively, whereas the Cluster-Based Normalization counterpart achieves a notably lower test error of **0.36**. Transitioning to the deeper DenseNet with 100 layers (DenseNet-100), the test errors for the BN and MN models drop to **0.3** and **0.29**, respectively,

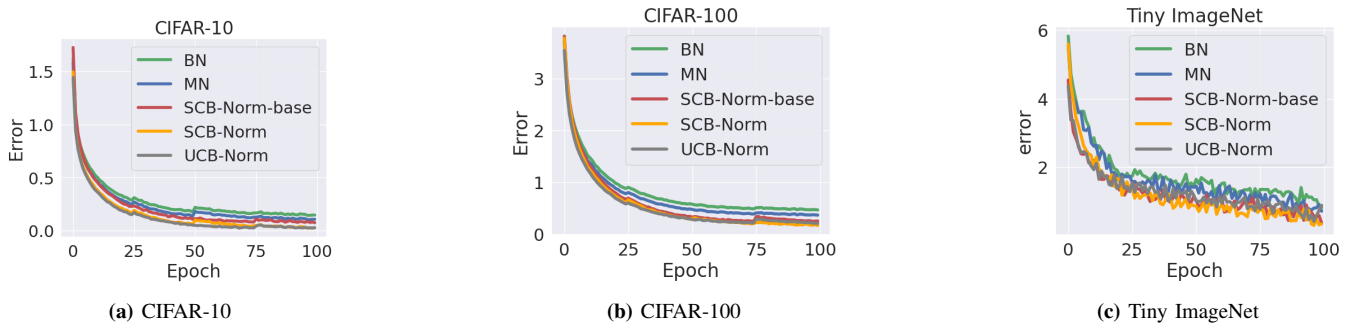


**Fig. 3:** Learning rate = 0.001

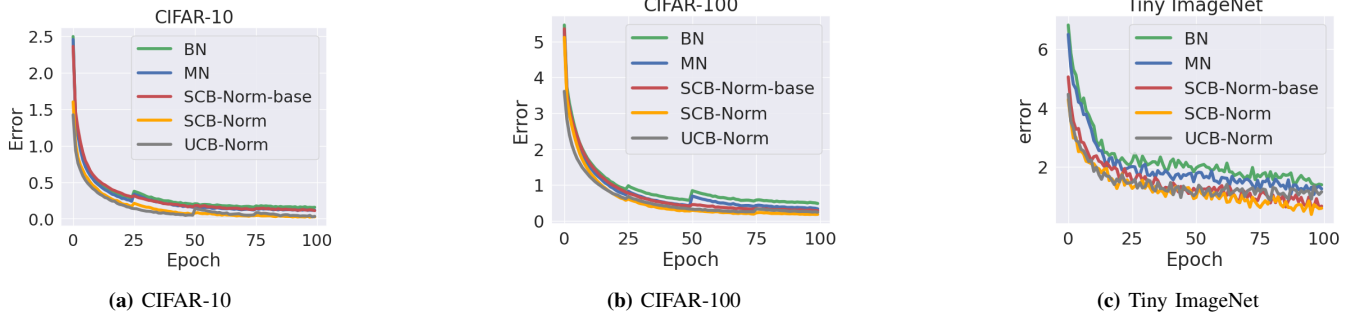


**Fig. 4:** Learning rate = 0.005

**Fig. 5:** Test error curves when Shallow CNN (detailed in Table IV) architecture is trained under different learning rate. We observe that on CIFAR-10, CIFAR-100 and Tiny ImageNet, Cluster-based Normalization method (SCB-Norm, SCB-Norm-base and UCB-Norm) performs consistently in both small and large learning rate regimes.

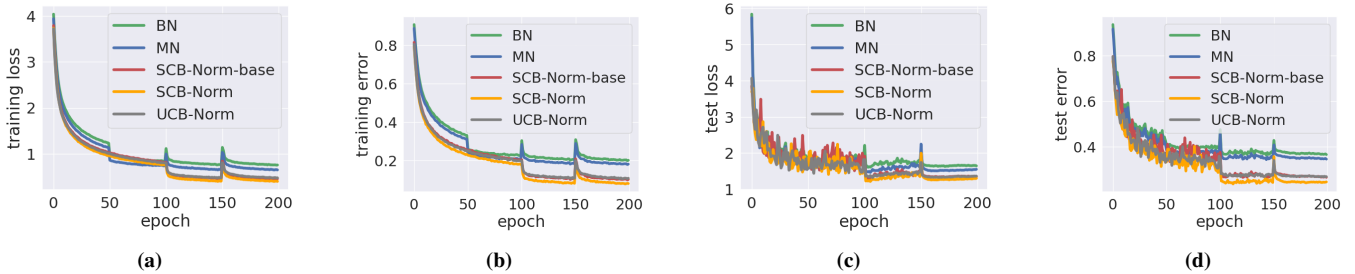


**Fig. 6:** DenseNet-40

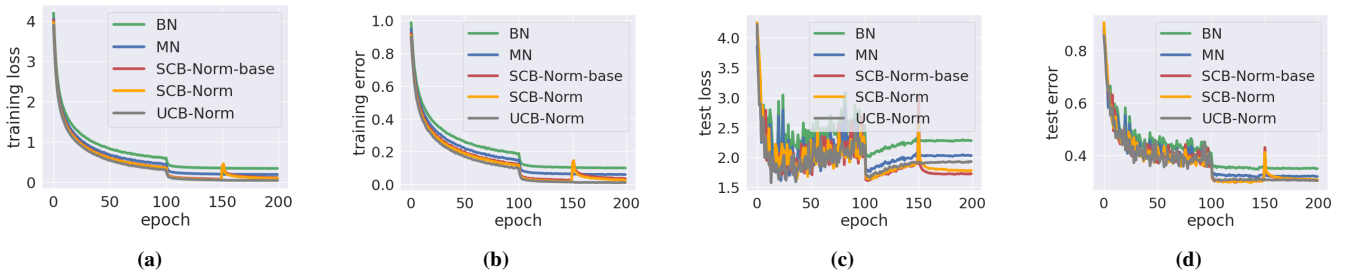


**Fig. 7:** DenseNet-100

**Fig. 8:** Experiments on CIFAR-100 using DenseNet [37] are showcased in Figure 6 and 7. The training/test error and cross-entropy loss are depicted for DenseNet with 40 layers (DenseNet-40) and DenseNet with 100 layers (DenseNet-100). Notably, the incorporation of CB-Norm (SCB-Norm-base, SCB-Norm, and UCB-Norm) significantly enhances the training process, expediting optimization. Concurrently, it demonstrates superior generalization, as evidenced by a consistently substantial margin compared to its batch normalized and mixture normalized counterparts in the error curve.

while the cluster-based normalization variants achieve the best test error of **0.28**.

In the following section, we will demonstrate a specialized

application of CB-Norm with the unsupervised version (UCB-Norm) in image generation.

| CIFAR-10        |               |              |              |              |              |
|-----------------|---------------|--------------|--------------|--------------|--------------|
| model           | learning rate | 25 epochs    | 50 epochs    | 75 epochs    | 100 epochs   |
| BN-1            | 0.001         | 84.34        | 86.49        | 86.41        | 86.90        |
| BN-2            | 0.005         | 83.44        | 84.39        | 85.65        | 85.65        |
| MN-1            | 0.001         | 84.45        | 86.60        | 86.6         | 87.07        |
| MN-2            | 0.005         | 83.47        | 84.60        | 85.68        | 85.80        |
| SCB-Norm-base-1 | 0.001         | <b>85.9</b>  | <b>86.93</b> | 87.09        | 87.11        |
| SCB-Norm-base-2 | 0.005         | 83.65        | 85.09        | 86.28        | 86.41        |
| SCB-Norm-1      | 0.001         | 84.68        | 86.61        | <b>87.38</b> | <b>87.57</b> |
| SCB-Norm-2      | 0.005         | 84.85        | <b>86.54</b> | <b>87.07</b> | 87.07        |
| UCB-Norm-1      | 0.001         | 85.15        | 85.80        | 87.97        | 87.97        |
| UCB-Norm-2      | 0.005         | <b>86.04</b> | 86.04        | <b>87.49</b> | <b>87.49</b> |

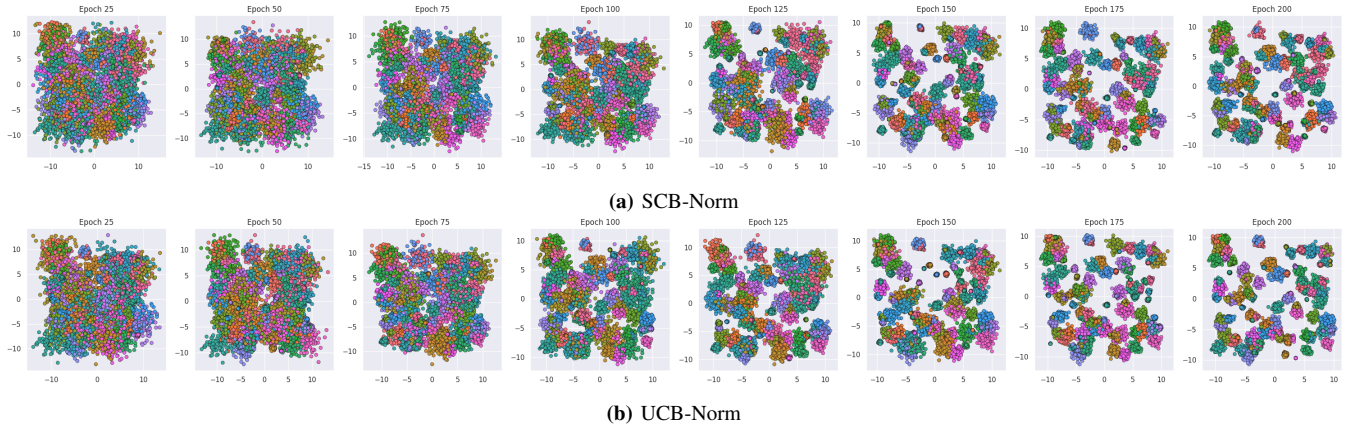
  

| CIFAR-100       |               |              |              |              |              |
|-----------------|---------------|--------------|--------------|--------------|--------------|
| model           | learning rate | 25 epochs    | 50 epochs    | 75 epochs    | 100 epochs   |
| BN-1            | 0.001         | 57.41        | 59.74        | 59.82        | 59.82        |
| BN-2            | 0.005         | 55.64        | 56.97        | 56.29        | 56.29        |
| MN-1            | 0.001         | 56.90        | 59.80        | 59.80        | 60.10        |
| MN-2            | 0.005         | 55.80        | 55.80        | 56.56        | 57.09        |
| SCB-Norm-base-1 | 0.001         | 57.74        | 61.01        | 61.01        | 61.01        |
| SCB-Norm-base-2 | 0.005         | 55.47        | 57.06        | 57.06        | 57.60        |
| SCB-Norm-1      | 0.001         | 58.50        | 59.25        | 59.65        | 61.02        |
| SCB-Norm-2      | 0.005         | 55.81        | 57.68        | 57.68        | 57.68        |
| UCB-Norm-1      | 0.001         | <b>59.44</b> | <b>61.10</b> | <b>61.10</b> | <b>61.10</b> |
| UCB-Norm-2      | 0.005         | <b>58.31</b> | <b>60.29</b> | <b>60.29</b> | <b>60.29</b> |

| Tiny ImageNet   |               |              |              |              |              |
|-----------------|---------------|--------------|--------------|--------------|--------------|
| model           | learning rate | 25 epochs    | 50 epochs    | 75 epochs    | 100 epochs   |
| BN-1            | 0.001         | 37.17        | 37.17        | 37.17        | 37.17        |
| BN-2            | 0.005         | 34.11        | 34.11        | 34.11        | 34.11        |
| MN-1            | 0.001         | 38.18        | 38.17        | 38.5         | 38.5         |
| MN-2            | 0.005         | 34.56        | 34.99        | 35.12        | 35.27        |
| SCB-Norm-base-1 | 0.001         | 38.53        | <b>40.08</b> | 40.08        | 40.08        |
| SCB-Norm-base-2 | 0.005         | 34.78        | 35.44        | 35.44        | 36.71        |
| SCB-Norm-1      | 0.001         | 37.72        | 39.45        | <b>40.29</b> | <b>40.29</b> |
| SCB-Norm-2      | 0.005         | <b>37.97</b> | <b>38.31</b> | <b>38.31</b> | <b>38.31</b> |
| UCB-Norm-1      | 0.001         | <b>39.71</b> | 39.71        | 39.71        | 39.71        |
| UCB-Norm-2      | 0.005         | 35.78        | 37.03        | 37.03        | 37.03        |

**TABLE V:** Evaluating Performance on CIFAR-10, CIFAR-100, and Tiny ImageNet Using the Shallow CNN architecture (see Table IV) with the Integration of Batch Normalization (BN), Mixture Normalization (MN), and Cluster-based Normalization (SCB-Norm-base, SCB-Norm and UCB-Norm). Each model is associated with a specific numerical identifier, denoting the learning rate.



**Fig. 9:** Visualization of Clustering Patterns in Activations: The t-SNE visualization of activations from models trained on CIFAR-100 with SCB-Norm and UCB-Norm normalization layers. The figure illustrates the formation of distinct clusters aligning with predicted target classes, showcasing improved clustering patterns over the course of training.

#### D. Unsupervised Cluster-based Normalization (UCB-Norm) Generative Adversarial Networks (GANs)

GANs, or Generative Adversarial Networks [39], are deep learning models used to generate realistic data, such as images [40]–[42]. The GAN architecture consists of two competing neural networks: a generator and a discriminator.

The generator creates data, while the discriminator evaluates its authenticity. The training process occurs through iterations, where the generator seeks to improve its ability to deceive the discriminator, while the discriminator aims to become more effective at distinguishing generated data from real data.

However, a common challenge encountered when using GANs is the issue of "mode collapse". This phenomenon occurs when the generator produces only a restricted subset of possible data, leading to a loss of diversity in the generated results. In other words, the generator may focus on producing a specific type of data, neglecting the generation of other potential variations. This problem can compromise the quality and variety of the generated data, requiring specific techniques and strategies to address and enhance the overall performance of the GAN model. UCB-Norm independently standardizes internal activations across diverse disentangled modes of variation, utilizing a normalization-based approach with multiple mixture components. We postulate that integrating this approach into the generator has the potential to markedly improve the training procedure of GANs.

To test our hypothesis, we examine the Deep Convolutional Generative Adversarial Network (DCGAN) [40], which is a dedicated GAN specifically crafted for image generation tasks. In the architecture we used, the generator is composed of a linear layer followed by four deconvolutional layers. The first three deconvolutional layers are succeeded by a batch normalization layer and then a LeakyReLU [43] activation function. In this setup, the linear layer likely serves as an initial mapping from a latent space to a higher-dimensional representation. The four deconvolutional layers, also known as transposed convolutional layers, work to upsample the input progressively, transforming it into a realistic output. Batch normalization is applied after the first three deconvolutional layers, aiding in stabilizing and expediting the training process. The LeakyReLU activation function introduces non-linearity, enabling the model to learn more intricate mappings. We replace the batch normalization layers associated with the first two deconvolution layers with mixture normalization (utilizing three mixture components) and unsupervised cluster-based normalization, also with  $K = 3$  mixture components. The training of all models is conducted on CIFAR-100 for 200 epochs, employing the Adam optimizer [36] with  $\alpha = 0.0002$ ,  $\beta_1 = 0$ , and  $\beta_2 = 0.9$  for both the generator and discriminator. The assessment of GAN quality is gauged using the "Fréchet Inception Distance" (FID) [44], calculated every 10 epochs for computational efficiency. Figure 10 illustrates that the DCGAN incorporating cluster-based normalization (DCGAN-UCB-Norm) exhibits not only a quicker convergence compared to its batch-normalized and mixture-normalized counterparts but also achieves superior (lower) Fréchet Inception Distance (FID) scores.

At the conclusion of the model training, Figure 11 displays examples of generated images produced by DCGANs with batch normalization, mixture normalization, and cluster-based normalization.

In the upcoming experiments, we will focus on practical approaches to constructing prior knowledge clusters in the case of SCB-Norm without relying on any specific algorithm.

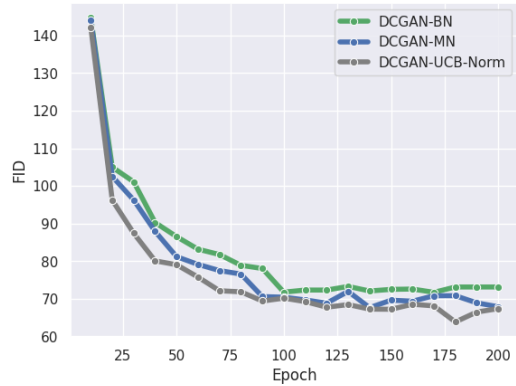


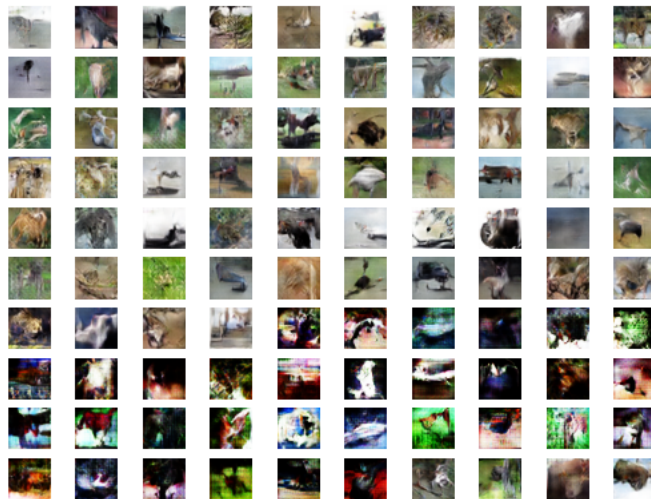
**Fig. 10:** Unsupervised Cluster-based Normalization (UCB-Norm) incorporated into the architecture of the deep Convolutional Generative Adversarial Network (DCGAN) [40]. Our findings indicate that integrating our proposed cluster-based normalization into the generator of DCGAN (DCGAN-UCB-Norm) enhances the efficiency of the training process. In contrast to the standard DCGAN employing batch normalization (DCGAN-BN) and DCGAN using mixture normalization (DCGAN-MN), DCGAN-UCB-Norm not only demonstrates accelerated convergence but also attains superior (lower) Fréchet Inception Distance (FID) scores.

This method enhances the applicability of the supervised version of CB-Norm. We will employ diverse neural network architectures to thoroughly explore the versatility. The mixture normalization, requiring data partitioning with the EM algorithm to find normalization parameters corresponding to the components, cannot be applied as a baseline.

#### E. Cluster-based Normalization In Domain Adaptation

In this experimental setup, we showcase how the effectiveness of cluster-based normalization in improving local representations can result in substantial advancements in domain adaptation. As elucidated in [45], domain adaptation entails harnessing knowledge acquired by a model from a related domain, where there is an ample amount of labeled data, to enhance the model's performance in a target domain characterized by limited labeled data. In this context, we consider two domains (clusters) ( $Z = K = 2$ ): the "source domain" and the "target domain". To exemplify this, we employ the two versions of cluster-based normalization (SCB-Norm with its variant SCB-Norm-base, and UCB-Norm) in conjunction with AdaMatch [34], a method that integrates the tasks of unsupervised domain adaptation (UDA), semi-supervised learning (SSL), and semi-supervised domain adaptation (SSDA). In UDA, we have access to a labeled dataset from the source domain and an unlabeled dataset from the target domain. The objective is to train a model capable of generalizing effectively to the target dataset. It's important to note that the source and target datasets exhibit variations in distribution. Specifically, we utilize the MNIST dataset as the source dataset, while the target dataset is SVHN. Both datasets encompass various factors of variation, including

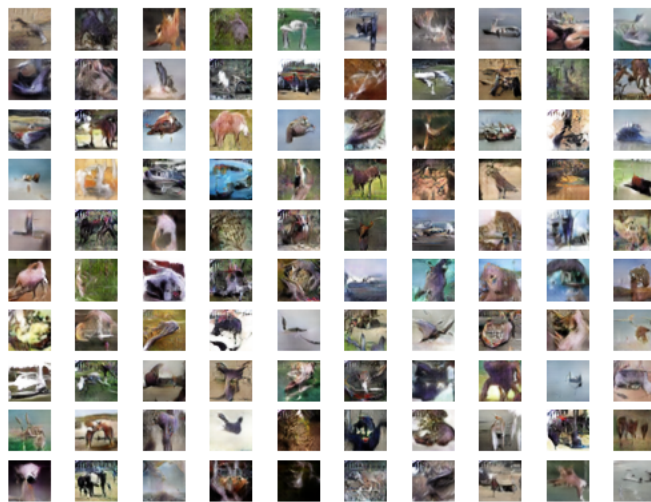




(a) DCGAN-BN



(b) DCGAN-MN



(c) DCGAN-UCB-Norm

**Fig. 11:** Examples of generated images at epoch 200 are showcased for DCGAN-BN, DCGAN-MN, and DCGAN-UCB-Norm in Figure 11a, 11b, and 11c, respectively.

| MNIST (source domain)  |              |              |              |              |
|------------------------|--------------|--------------|--------------|--------------|
| model                  | accuracy     | precision    | recall       | f1-score     |
| AdaMatch               | 97.36        | 87.33        | 79.39        | 78.09        |
| AdaMatch+SCB-Norm-base | <b>99.26</b> | <b>99.20</b> | <b>99.32</b> | <b>99.26</b> |
| AdaMatch+SCB-Norm      | 98.92        | 98.93        | 98.92        | 98.92        |
| AdaMatch+UCB-Norm      | 98.9         | 98.5         | 98.90        | 98.95        |
| SVHN (target domain)   |              |              |              |              |
| model                  | accuracy     | precision    | recall       | f1-score     |
| AdaMatch               | 25.08        | 31.64        | 20.46        | 24.73        |
| AdaMatch+SCB-Norm-base | 43.10        | 53.83        | 43.10        | 47.46        |
| AdaMatch+SCB-Norm      | <b>54.70</b> | <b>59.74</b> | <b>54.70</b> | <b>54.55</b> |
| AdaMatch+UCB-Norm      | 33.4         | 43.83        | 40.28        | 42.87        |

**TABLE VI:** Comparing model performance: AdaMatch vs. AdaMatch+SCB-Norm-base, AdaMatch+SCB-Norm and AdaMatch+UCB-Norm on MNIST (source) and SVHN (target) datasets.

texture, viewpoint, appearance, etc., and their domains, or distributions, are distinct from each other.

A model, referred to as AdaMatch [46] (using batch normalization as normalization), is trained from the ground up using wide residual networks [47] on pairs of datasets, serving as the baseline model. The training of this model involves utilizing the Adam optimizer [36] with a cosine decay schedule, gradually reducing the initial learning rate initialized at 0.03. SCB-Norm, SCB-Norm-base, and UCB-Norm are incorporated as initial layers in AdaMatch, leading to the creation of three AdaMatch models based on cluster-based normalization (AdaMatch+SCB-Norm, AdaMatch+SCB-Norm-base, and AdaMatch+UCB-Norm). This integration allows the cluster identifier (source domain and target domain) to influence the image normalization process. Since the labels in the source domain are known, the model can offer a more accurate representation of this domain in comparison to the target domain where the labels are unknown. This advantageous aspect is harnessed by considering the cluster identifier of the source domain during inference in AdaMatch+SCB-Norm and AdaMatch+SCB-Norm-base, thereby improving the model’s performance on the target domain.

Undoubtedly, within a wider context, Table VI unequivocally highlights a remarkable enhancement in validation metrics attributable to the incorporation of cluster-based normalization. This advancement is conspicuous, manifesting as a substantial boost in accuracy by **18.02%** with SCB-Norm-base, **29.62%** with SCB-Norm, and **8.32%**. Such marked improvement notably fortifies the performance of the AdaMatch model, leading to a significantly expedited convergence during training. The difference in performance between the supervised approach (SCB-Norm and its variant SCB-Norm-base) and the unsupervised approach (UCB-Norm) can be explained by the fact that SCB-Norm takes prior knowledge information (clusters that are source and target domains), as input and directly integrates it into the normalization process. This allows for a specific representation for each domain. In contrast, UCB-Norm does not take prior knowledge as input but only considers the number of mixture components to be estimated, which is  $K = 2$ . Estimating mixture components

in this manner can be challenging in this use case, as the information from each component is incorporated into all images, regardless of their domain. This can strongly influence the representation of the data and consequently impact performance. Figure 12 visually underscores the invaluable contribution of cluster-based normalization through SCB-Norm in stabilizing the gradient across the entire training process, yielding benefits for both the source and target domains. Consequently, this stabilization significantly contributes to accelerated convergence and an overall enhancement in model performance.

In the following experiment, we will demonstrate another approach to construct prior knowledge (clusters) on supervised version (SCB-Norm) on a Vision Transformer [48] and then on a Convolutional Neural Network (CNN).

#### F. Supervised Cluster-based Normalization (SCB-Norm) Using Superclasses As Prior Knowledge

As delineated in Section IV-A, both the CIFAR-100 dataset and the Oxford-IIIT Pet dataset incorporate a superclass structure alongside their class divisions. In our proposed supervised cluster-based normalization approach, we harness this superclass information as “prior knowledge” for classification tasks. Specifically, each superclass is treated as a distinct cluster. We have incorporated the adaptive normalization technique into the Vision Transformer (ViT) architecture for CIFAR-100 classification. For our ViT implementation, we utilized a Keras baseline provided by [49]. Additionally, for the Oxford-IIIT Pet dataset, we adopted a Convolutional Neural Network (CNN) architecture as our baseline, as described in [50].

1) *Using CIFAR-100 Superclass as Prior Knowledge in supervised cluster-based normalization:* The central innovation in this experiment revolves around utilizing CIFAR-100 superclasses as prior knowledge (clusters) for predicting the dataset’s 100 classes, particularly in the case of SCB-Norm-base and SCB-Norm methods.

Three distinct models were employed: the base ViT model obtained from Keras [49], a modified version incorporating a Batch Normalization (BN) layer as its initial component, and two alternative models that replaced the BN layer with SCB-Norm-base and SCB-Norm layers. Training included early stopping based on validation performance, and images were pre-processed by normalizing them with respect to the dataset’s mean and standard deviation. Data augmentation techniques, such as horizontal flipping and random cropping, were applied to enhance the dataset. The AdamW optimizer, with a learning rate of  $10^{-3}$  and a weight decay of  $10^{-4}$ , was chosen to prevent overfitting and optimize model parameters [35, 36]. Table VII presents the notable performance enhancements achieved by our innovative Supervised Cluster-based Normalization (SCB-Norm and its variant SCB-Norm-base) in comparison to training the ViT architecture from scratch on CIFAR-100 with Batch Normalization (BN). The SCB-Norm approach

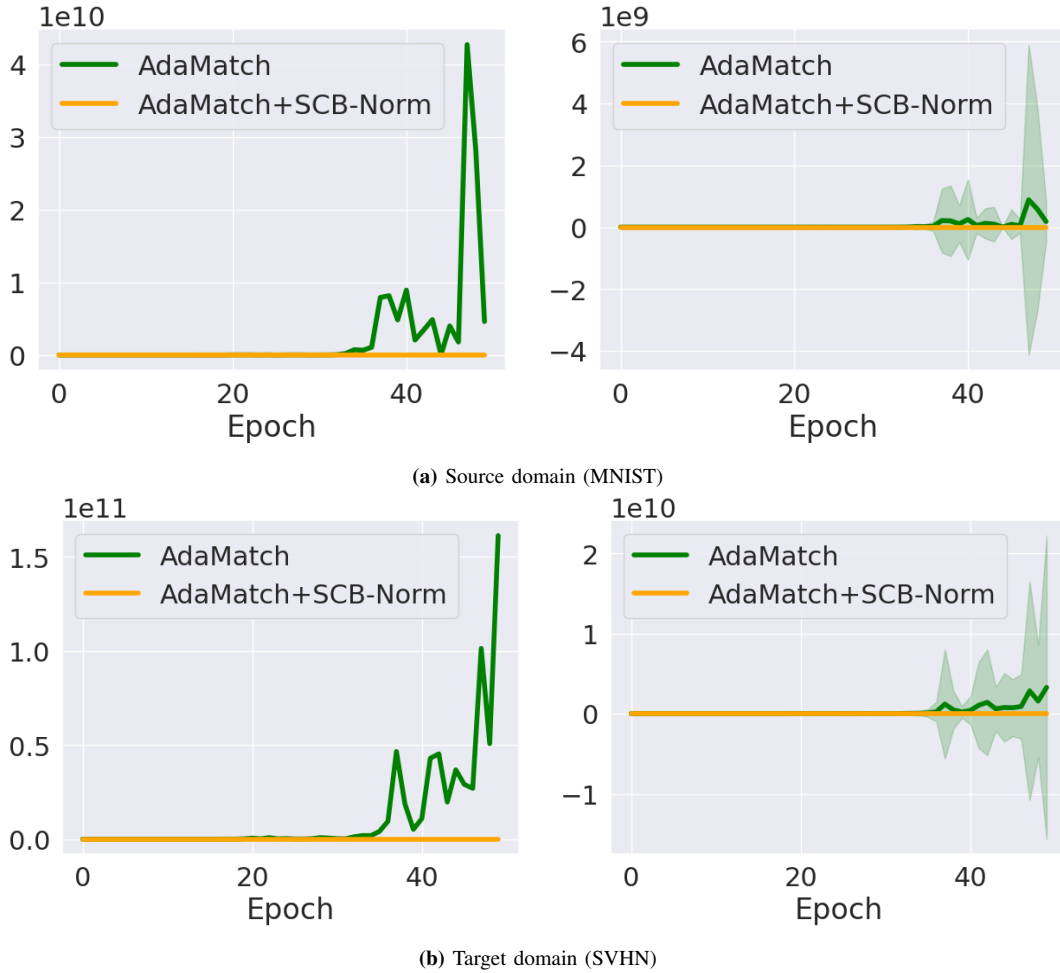


**Fig. 12:** Evolution of the gradient variance during the training of AdaMatch and AdaMatch+SCB-Norm models on the source (MNIST) and target (SVHN) domains. The figures on the left correspond to the maximum gradient variance for each epoch, while the figures on the right correspond to the average gradient variance per epoch.

| model             | accuracy     | precision    | recall       | f1-score     |
|-------------------|--------------|--------------|--------------|--------------|
| ViT+BN            | 55.63        | 8.96         | 90.09        | 54.24        |
| ViT+SCB-Norm-base | 65.87        | <b>23.36</b> | 98.53        | 65.69        |
| ViT+SCB-Norm      | <b>67.38</b> | <b>22.93</b> | <b>99.00</b> | <b>67.13</b> |

**TABLE VII:** Assessing the Performance of CIFAR-100 Using the ViT Architecture [49] incorporating BN, SCB-Norm-base, and SCB-Norm, with CIFAR-100 superclasses serving as prior knowledge or clusters.

demonstrates an accuracy improvement of approximately **12%** over BN. Furthermore, it is noteworthy that both SCB-Norm-base and SCB-Norm exhibit faster convergence compared to BN, requiring less training time to attain superior performance. This observation is further supported by the comparison of train and validation loss depicted in Figure 13, indicating that SCB-Norm promotes accelerated learning while improving classification performance. These findings suggest that the proposed SCB-Norm method not only stabilizes data distributions and mitigates internal covariate shift but also significantly reduces training time for enhanced results. ViT+SCB-Norm-base and ViT+SCB-Norm achieve outstanding performance, surpassing all known ViT

models when trained from scratch on the CIFAR-100 dataset.

After training the ViT model with the SCB-Norm layer (ViT+SCB-Norm), it is applied to a randomly selected batch of data to analyze the effect of SCB-Norm on the representation of data according to prior knowledge (superclasses using as distinct clusters). After retrieving the outputs, Principal Component Analysis (PCA) is applied, with 5 components, to visualize the behavior of our supervised cluster-based normalization method. Figure 14 illustrates this approach, showing a representation of data according to prior knowledge. The emerging cluster structure provides a better representation, thereby contributing to class separation and facilitating prediction.

2) *Using Oxford-IIIT Superclass as Prior Knowledge in supervised cluster-based normalization:* In this experiment, mirroring the one in the preceding section with CIFAR-100, we leverage the superclasses (dog and cat) from the Oxford-IIIT Pet Dataset to classify the 37 categories within the dataset. In this methodology, we employ a CNN (OxfordCNN) as the foundational model [50] and

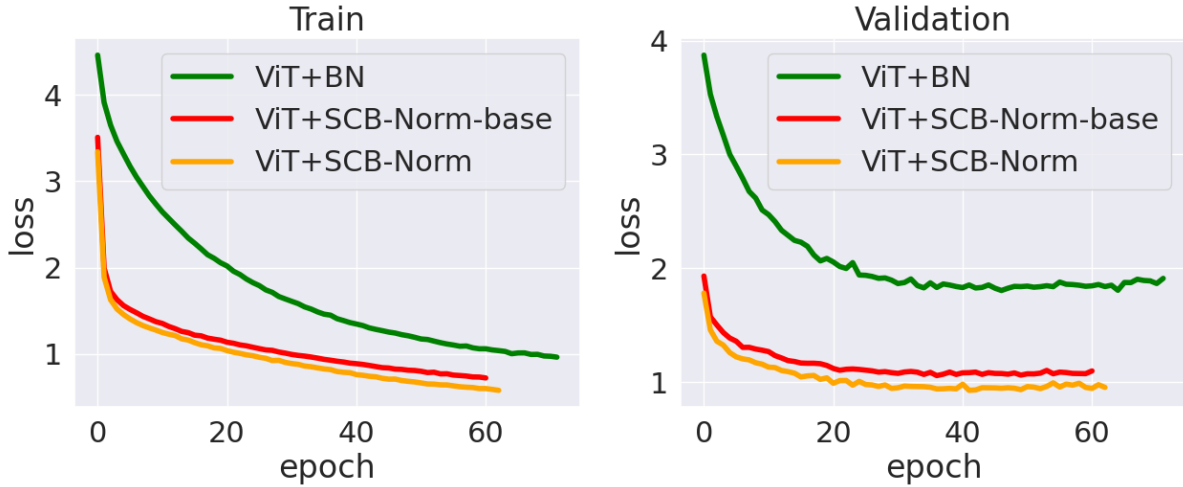


**Fig. 13:** Contrasting Training and Validation Loss Curves: Within the ViT Architecture on CIFAR-100, SCB-Norm and SCB-Norm-base exhibit swifter convergence and reduced validation loss, enhancing learning efficiency and classification performance compared to BN.

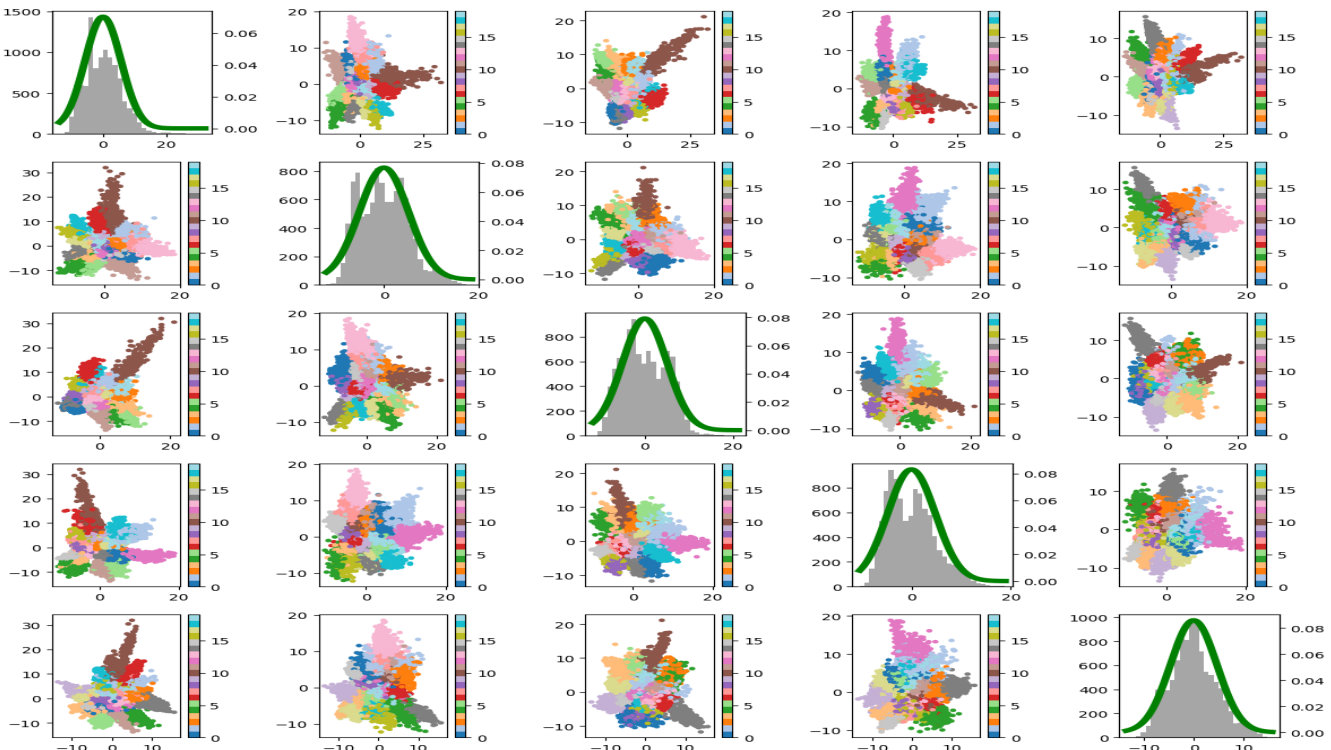


**Fig. 14:** Projection of ViT+SCB-Norm outputs after applying Principal Component Analysis (PCA) for dimension reduction. Coloring is based on superclasses. A clear separation is observed between the superclasses, representing the prior knowledge (clusters). This separation leads to an enhanced representation, significantly facilitating the classification task. The green line on the histograms corresponds to the probability density function (pdf).

integrate our SCB-Norm layer just before the neural network’s prediction layer (linear layer). This experiment illustrates that supervised cluster-based normalization can function as a layer at various levels of the neural network, thereby enhancing both performance and convergence. The models underwent training for 200 epochs with early stopping criteria based on validation performance. Image preprocessing involved normalization using the mean and standard deviation of the dataset. Data augmentation

techniques, including horizontal flipping and random cropping, were employed to enhance the dataset. The training utilized the Adam optimizer [36] with a learning rate of  $10^{-4}$ .

The results presented in Table VIII reinforce the earlier observations with CIFAR-100. It is apparent that cluster-based normalization leads to significantly faster convergence, a trend further supported by the performance achieved by SCB-Norm. SCB-Norm reaches a



| Model                   | Epoch     | Metrics      |              |              |              |
|-------------------------|-----------|--------------|--------------|--------------|--------------|
|                         |           | Accuracy     | Precision    | Recall       | F1-Score     |
| OxfordCNN base          | Epoch 80  | 63.12        | 50.23        | 80.11        | 69.23        |
|                         | Epoch 113 | 66.55        | 53.11        | 84.2         | 72.15        |
| OxfordCNN+SCB-Norm-base | Epoch 80  | 64.90        | 52.34        | 83.10        | 73.11        |
|                         | Epoch 113 | 67.52        | 55.12        | 86.13        | 75.90        |
| OxfordCNN+SCB-Norm      | Epoch 80  | <b>67.92</b> | <b>54.24</b> | <b>89.11</b> | <b>80.12</b> |
|                         | Epoch 113 | <b>73.61</b> | <b>69.12</b> | <b>92.34</b> | <b>90.11</b> |

**TABLE VIII:** Assessing Performance on the Oxford-IIIT Pet Dataset Using the OxfordCNN Architecture [50], incorporating SCB-Norm-base and SCB-Norm with "dog" and "cat" superclasses serving as prior knowledge (distinct clusters).

performance level after 80 epochs that surpasses the baseline (OxfordCNN), which takes 113 epochs to reach convergence.

## V. CONCLUSION

Cluster-based Normalization (CB-Norm) emerges as a groundbreaking one-step normalization method, addressing challenges in neural network training. Its adaptability and unique approach, incorporating Gaussian mixture models, mark a significant advancement in overcoming issues like internal covariate shift and gradient stability. Through Supervised Cluster-based Normalization (SCB-Norm) and Unsupervised Cluster-based Normalization (UCB-Norm), CB-Norm demonstrates versatility in handling diverse learning scenarios. SCB-Norm utilizes predefined data partitioning (clusters), while UCB-Norm incrementally clusters activations without using prior knowledge, both contributing to enhanced adaptability. Our experiments aim to assess CB-Norm's performance, comparing it with Batch Normalization (BN) and Mixture Normalization (MN). We apply SCB-Norm and UCB-Norm to various tasks, including classification, domain adaptation, and generative neural networks. Furthermore, we introduce SCB-base, a simplified variant, maintaining a fixed cluster identifier ( $z$ ) and leveraging neural networks to encode cluster information. These experiments collectively aim to showcase the efficacy and versatility of CB-Norm in improving neural network performance across a spectrum of applications. Importantly, it's worth noting that CB-Norm drastically reduces computation complexity compared to BN and MN, further enhancing its appeal for practical implementation in real-world scenarios.

## REFERENCES

- [1] A. Kessy, A. Lewin, and K. Strimmer, "Optimal whitening and decorrelation," *The American Statistician*, vol. 72, no. 4, pp. 309–314, 2018.
- [2] Y. LeCun, L. Bottou, G. B. Orr, and K.-R. Müller, "Efficient backprop," in *Neural networks: Tricks of the trade*, pp. 9–50, Springer, 2002.
- [3] S. Ioffe and C. Szegedy, "Batch normalization: Accelerating deep network training by reducing internal covariate shift," in *International conference on machine learning*, pp. 448–456, PMLR, 2015.
- [4] L. Huang, J. Qin, Y. Zhou, F. Zhu, L. Liu, and L. Shao, "Normalization techniques in training dnns: Methodology, analysis and application," *arXiv preprint arXiv:2009.12836*, 2020.
- [5] J. L. Ba, J. R. Kiros, and G. E. Hinton, "Layer normalization," *arXiv preprint arXiv:1607.06450*, 2016.
- [6] Y. Wu and K. He, "Group normalization," in *Proceedings of the European conference on computer vision (ECCV)*, pp. 3–19, 2018.
- [7] D. Ulyanov, A. Vedaldi, and V. Lempitsky, "Instance normalization: The missing ingredient for fast stylization," *arXiv preprint arXiv:1607.08022*, 2016.
- [8] Q. Wang, Y. Wu, L. Li, and W. Liu, "Multi-batch normalization," *arXiv preprint arXiv:2002.05712*, 2020.
- [9] Y. Li, S. X. Yu, K. Li, T. Chai, and Y. Lin, "Group normalization with modulation," *arXiv preprint arXiv:2005.11258*, 2020.
- [10] M. Tan, B. Chen, R. Pang, V. Vasudevan, M. Sandler, A. Howard, and Q. V. Le, "Efficientnetv2: Smaller models and faster training," *arXiv preprint arXiv:2104.00298*, 2020.
- [11] P. Zhang, J. Wang, Z. Sun, and S. Ren, "Adabn: Adaptive batch normalization for improving generalization of deep networks," *arXiv preprint arXiv:2006.14609*, 2020.
- [12] P. Zhang, J. Wang, Z. Sun, and S. Ren, "Rbn: Random batch normalization for training very deep neural networks," *arXiv preprint arXiv:2006.15840*, 2020.
- [13] C. Liu, T. He, B. Wang, M. Andriushchenko, M. Belkin, and J. Long, "Adaptive normalization for out-of-distribution generalization," *arXiv preprint arXiv:2011.14162*, 2020.
- [14] Y. He, X. Dong, Q. Wen, J. Zhang, N. Yu, and R. Chen, "Momentum batch normalization," *arXiv preprint arXiv:2010.14627*, 2020.
- [15] W. Mao, J. Wang, and Y. Xiong, "Cross-layer batch normalization," *arXiv preprint arXiv:2011.01932*, 2020.
- [16] Q. Huang, P. Li, Y. Lyu, and L. Liang, "Batch spectral regularization for improving generalization of deep neural networks," *arXiv preprint arXiv:2011.01971*, 2020.
- [17] W. Jiang and Z.-H. Zhou, "Graph-based batch normalization," *arXiv preprint arXiv:2101.08458*, 2021.
- [18] H. B. Kim, J. Jeon, and H. O. Kim, "Instance-dependent batch normalization," *arXiv preprint arXiv:2012.07946*, 2020.
- [19] K. Han, Y. Wang, Q. Zhang, W. Xu, and J. Sun, "Msr-mixer: Mixture-of-skip-residual blocks for efficient vision transformers," *arXiv preprint arXiv:2109.14787*, 2021.
- [20] D. Wang, J. Lu, and D. Wang, "Searching batch normalization algorithms," *arXiv preprint arXiv:2110.01101*, 2021.
- [21] M. Zhang, Z. Li, and J. Zhang, "Instance normalization with batch normalization," *arXiv preprint arXiv:2111.09409*, 2021.
- [22] L. Wang and H. Zhu, "Smallest achievable batch normalization," *arXiv preprint arXiv:2111.12068*, 2021.
- [23] J. Wu, L. Yao, J. Zhang, Z. Zhang, K. Huang, J. Xu, X. Zhang, J. Yang, and Q. Xie, "Token-batch normalization: Towards efficient normalization and attention fusion in vision transformers," *arXiv preprint arXiv:2203.06751*, 2022.
- [24] M. M. Kalayeh and M. Shah, "Training faster by separating modes of variation in batch-normalized models," *IEEE transactions on pattern analysis and machine intelligence*, vol. 42, no. 6, pp. 1483–1500, 2019.
- [25] A. P. Dempster, N. M. Laird, and D. B. Rubin, "Maximum likelihood from incomplete data via the EM algorithm," *JOURNAL OF THE ROYAL STATISTICAL SOCIETY, SERIES B*, vol. 39, no. 1, pp. 1–38, 1977.
- [26] V. Dumoulin, J. Shlens, and M. Kudlur, "A learned representation for artistic style," *arXiv preprint arXiv:1610.07629*, 2016.
- [27] X. Huang, M.-Y. Liu, S. Belongie, and J. Kautz, "Multimodal unsupervised image-to-image translation," in *Proceedings of the European conference on computer vision (ECCV)*, pp. 172–189, 2018.
- [28] D. Arthur and S. Vassilvitskii, "k-means++: The advantages of careful seeding," *Proceedings of the eighteenth annual ACM-SIAM symposium on Discrete algorithms*, pp. 1027–1035, 2007.

- [29] A. Krizhevsky, V. Nair, and G. Hinton, "CIFAR-10 (canadian institute for advanced research)," 2009.
- [30] A. Krizhevsky, V. Nair, and G. Hinton, "CIFAR-100 (canadian institute for advanced research)," 2009.
- [31] Y. Le and X. Yang, "Tiny imagenet visual recognition challenge," *CS 231N*, vol. 7, no. 7, p. 3, 2015.
- [32] Y. LeCun and C. Cortes, "MNIST handwritten digit database," 2010.
- [33] P. Sermanet, S. Chintala, and Y. LeCun, "Convolutional neural networks applied to house numbers digit classification," in *Proceedings of the 21st international conference on pattern recognition (ICPR2012)*, pp. 3288–3291, IEEE, 2012.
- [34] D. Berthelot, R. Roelofs, K. Sohn, N. Carlini, and A. Kurakin, "Adamatch: A unified approach to semi-supervised learning and domain adaptation," *arXiv preprint arXiv:2106.04732*, 2021.
- [35] I. Loshchilov and F. Hutter, "Decoupled weight decay regularization," *arXiv preprint arXiv:1711.05101*, 2017.
- [36] D. P. Kingma and J. Ba, "Adam: A method for stochastic optimization," *arXiv preprint arXiv:1412.6980*, 2014.
- [37] G. Huang, Z. Liu, L. Van Der Maaten, and K. Q. Weinberger, "Densely connected convolutional networks," in *Proceedings of the IEEE conference on computer vision and pattern recognition*, pp. 4700–4708, 2017.
- [38] Y. Bengio, N. Boulanger-Lewandowski, and R. Pascanu, "Advances in optimizing recurrent networks," in *2013 IEEE international conference on acoustics, speech and signal processing*, pp. 8624–8628, IEEE, 2013.
- [39] I. Goodfellow, J. Pouget-Abadie, M. Mirza, B. Xu, D. Warde-Farley, S. Ozair, A. Courville, and Y. Bengio, "Generative adversarial nets," *Advances in neural information processing systems*, vol. 27, 2014.
- [40] A. Radford, L. Metz, and S. Chintala, "Unsupervised representation learning with deep convolutional generative adversarial networks," *arXiv preprint arXiv:1511.06434*, 2015.
- [41] C. Ledig, L. Theis, F. Huszár, J. Caballero, A. Cunningham, A. Acosta, A. Aitken, A. Tejani, J. Totz, Z. Wang, *et al.*, "Photo-realistic single image super-resolution using a generative adversarial network," in *Proceedings of the IEEE conference on computer vision and pattern recognition*, pp. 4681–4690, 2017.
- [42] P. Isola, J.-Y. Zhu, T. Zhou, and A. A. Efros, "Image-to-image translation with conditional adversarial networks," in *Proceedings of the IEEE conference on computer vision and pattern recognition*, pp. 1125–1134, 2017.
- [43] A. L. Maas, A. Y. Hannun, and A. Y. Ng, "Rectifier nonlinearities improve neural network acoustic models," *arXiv preprint arXiv:1303.5778*, 2013.
- [44] M. Heusel, H. Ramsauer, T. Unterthiner, B. Nessler, and S. Hochreiter, "Gans trained by a two time-scale update rule converge to a local nash equilibrium," in *Advances in Neural Information Processing Systems*, 2017.
- [45] A. Farahani, S. Voghoei, K. Rasheed, and H. R. Arabnia, "A brief review of domain adaptation," *Advances in Data Science and Information Engineering: Proceedings from ICDATA 2020 and IKE 2020*, pp. 877–894, 2021.
- [46] S. Paul, "Unifying semi-supervised learning and unsupervised domain adaptation with adamatch," 2019. <https://github.com/keras-team/keras-io/tree/master>.
- [47] S. Zagoruyko and N. Komodakis, "Wide residual networks," *arXiv preprint arXiv:1605.07146*, 2016.
- [48] A. Dosovitskiy, L. Beyer, A. Kolesnikov, D. Weissenborn, X. Zhai, T. Unterthiner, M. Dehghani, M. Minderer, G. Heigold, S. Gelly, *et al.*, "An image is worth 16x16 words: Transformers for image recognition at scale," *arXiv preprint arXiv:2010.11929*, 2020.
- [49] K. Salama, "Implementing the vision transformer (vit) model for image classification," 2021. <https://github.com/keras-team/keras-io/tree/master>.
- [50] M. Garg, "Pet image classification," 1021. <https://github.com/mayur7garg>.